

## Some Evidence of Scaling Behavior in the Relaxation Dynamics of Aqueous Polymer Solutions

M. Pochylski,<sup>\*,†</sup> F. Aliotta,<sup>\*,‡</sup> R. C. Ponterio,<sup>‡</sup> F. Saija,<sup>‡</sup> and J. Gapiński<sup>†</sup>

Department of Physics, Adam Mickiewicz University, Poznań, Poland, and Istituto per I Processi Chimico Fisici del CNR, sezione di Messina, Italy

Received: June 04, 2009; Revised Manuscript Received: November 13, 2009

The structural relaxation behavior of aqueous solution of poly(ethylene glycol) and methoxy-capped poly(ethylene glycol), both of mean molecular mass 400 g/mol, is investigated by Brillouin scattering experiments. In both cases non-Debye relaxation processes have been detected, proceeding on the picosecond time scale. The average values of the detected relaxation time distributions fail to follow the simple Arrhenius behavior. The temperature evolution of the relaxation time is adequately fitted using the phenomenological Vogel–Fulcher–Tamman (VFT) model. In spite of the different temperature and concentration dependences observed for the two kinds of systems, with the exception of the highest samples concentrations, a unique scaling behavior has been found for the real and imaginary parts of the loss modulus plotted as a function of the reduced inverse temperature,  $T_0/T$ ,  $T_0$  being the VFT arrest temperature. The presence of a unique scaling law in aqueous solutions of polymers characterized by different end groups suggests the establishment of similar hydrogen-bonded local structures. Within this scenario, water acts as a *stabilizer* and plays the main role bridging neighboring polymer chains. The possible physical interpretation of the obtained fit parameters is discussed, and the results are compared with other literature findings.

### 1. Introduction

Aqueous solutions of relatively small amphiphilic molecules can be used as model systems to understand how hydrogen bond interaction can produce mesoscopic structures that are robust against the system composition over a wide range of temperatures.

The hydrogen bond between water molecules accounts for the many unusual behaviors observed in its liquid phase. As a result of hydrogen bonding, water can self-arrange in a variety of ways to form a sort of extended network with a bond density close to that observed in the ice phase. Since the binding and the thermal energies are of the same magnitude, the properties of liquid water depend on the half-life of hydrogen bonds rather than on their actual number. In addition, the existence of hydrogen bonding implies a sort of cooperativity in the system properties. Once a hydrogen bond is formed, the probability of developing a second bond may be substantially increased, similarly as in a catalytic reaction. This can produce a very strong and stable structure even though it is made up of individually weak bonds. This phenomenon plays the main role in maintaining both the structure and the function of any biological system. Molecular biology postulates a lower size limit for macromolecule (enzyme) aggregates in order to ensure their vital functions.<sup>1</sup> This condition was for the first time postulated by Schrödinger<sup>2</sup> who pointed out that in a living organism molecules have to cooperate. This requires a coordination over volumes large enough to avoid the effect of structure violation by thermal agitation. The *dissipative structures* theory<sup>3</sup> shows that the size of such self-assembled aggregates must exceed the spatial range of their Brownian diffusion during their lifetime. From this point of view, the crucial property of proteins

is their amphiphilic nature: the hydrophilic moieties attract water molecules while the hydrophobic ones repel them and, as a consequence, a complex hydrogen bond network is generated.

Poly(ethylene glycol) (PEG)–water mixtures are widely investigated<sup>4–12</sup> due to their technological relevance in many practical fields like gelation processes, water treatment, cosmetics, oral care, fibers, controlled drug delivery, etc. The polymeric chain of PEG is composed of alternating hydrophilic and hydrophobic groups, and so after addition of water it is able to exhibit a number of structural arrangements, which are not accessible to its anhydrous phase. As an example, the interaction with water can lead to a helical structure under specific conditions of concentration and temperature.<sup>9</sup> These properties and a simple molecular structure make PEG a very good model system for the study of water structuring effects in macromolecular solutions.

Brillouin spectroscopy allows to investigate the correlation between local structuring effects and hyperacoustic relaxations. Aqueous solutions of PEG of mean molecular mass of 600 g/mol (PEG600) have been already investigated by this technique<sup>4</sup> and a non-Arrhenius behavior of the relaxation time has been observed. This occurrence suggested for a distribution of relaxation times corresponding to a *fragile*<sup>13</sup> character of the system, according to the approach commonly used for glass forming liquids.

The possibility of substituting one of the two end groups of PEG chain offers the opportunity of testing the effects of the interaction with water, when similar polymeric chains with different water and self-affinity are compared.

In this work, we present the results of a Brillouin scattering experiment on PEG400/water mixtures and mixtures of water and methoxy capped PEG of the same molecular weight (poly(ethylene glycol) dimethyl ether, PEGDME400). The investigation of the relaxation dynamics in the two different systems will allow to infer how the presence of water induces

\* Corresponding authors. E-mail: pochyl@amu.edu.pl (M.P.); aliotta@me.cnr.it (F.A.).

<sup>†</sup> Adam Mickiewicz University.

<sup>‡</sup> Istituto per I Processi Chimico Fisici del CNR.

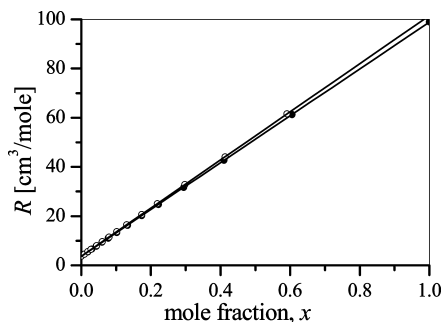


**Figure 1.** Mole fraction dependencies of the molar refraction  $R$  for aqueous solutions of PEG400 (full circles) and PEGDME400 (open circles). The whole sets of data at  $T = 25, 60$ , and  $90\text{ }^{\circ}\text{C}$  are reported. The error bars are systematically smaller than the size of the markers.

large structuring effects resulting in a collective behavior that is mainly governed by the kinetic of the hydrogen-bond network. In addition, we will show that such a water-induced behavior is largely independent of the specific polymer under consideration over wide frequency and temperature ranges.

## 2. Experimental Section

Poly(ethylene glycol) and poly(ethylene glycol) dimethyl ether, both of mean molecular mass  $400\text{ g/mol}$ , were obtained from Fluka Chemie GmbH and were used without any further purification procedure. Polydispersities of the two samples were comparable (1.19 for PEG and 1.15 for PEGDME). The melting point was experimentally estimated to be about  $270\text{ K}$  for both polymers. Binary mixtures of PEG400 and PEGDME400 in double distilled and deionized water were prepared as equidistant weight fractions, covering the whole concentration range from pure polymer to pure solvent. The concentration scale was then recalculated to monomer molar fraction,  $x'$ , defined as

$$x' = \frac{n_{\text{OE}}}{n_{\text{OE}} + n_{\text{solv}}} \quad (1)$$

$n_{\text{OE}}$  being the mean number of oxyethylene units of PEG or PEGDME chains in solution and  $n_{\text{solv}}$  the number of the solvent molecules.

The refractive index values,  $n$ , for each mixture were measured using a standard Pulfrich refractometer in the temperature range  $263\text{--}333\text{ K}$  (the temperature range accessible by our instrumentation). The values at temperatures outside the measured range were estimated by linear extrapolation of the experimental data.

The temperature and concentration dependencies of the density,  $\rho$ , were calculated using the refraction index data and the Lorentz–Lorenz relation:

$$\rho(T, x) = \frac{n(T, x)^2 - 1}{n(T, x)^2 + 2} \frac{M(x)}{R(x)} \quad (2)$$

where  $x$  stands for the molar fraction,  $M$  is the molar mass of the binary solution, and  $R$  is its molar refraction. This procedure is justified by the observation that, for aqueous solution of PEG and PEGDME, the molar refraction scales linearly with the polymer molar fraction and is apparently independent of temperature (Figure 1).

The Brillouin scattering measurements were performed on pure polymers and on their aqueous binary mixtures at three selected monomer molar fractions, namely  $x' = 0.33, 0.50$ , and  $0.66$  (corresponding to the polymer molar fractions  $x = 0.06$ ,

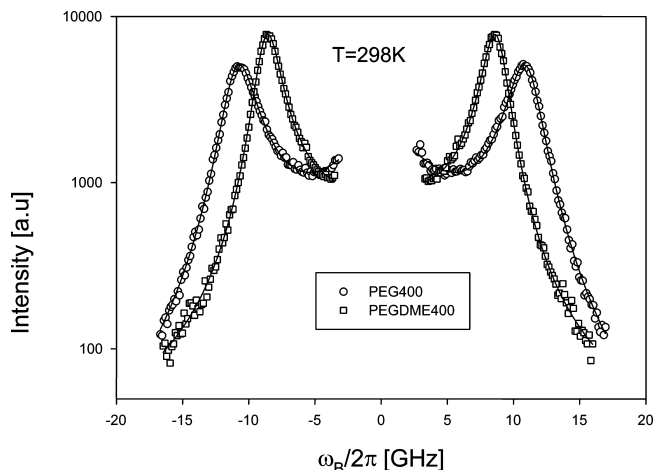


**Figure 2.** Experimental Brillouin spectra for PEG400 and PEGDME400 at  $298\text{ K}$ . Only one-third of the overall data points are shown for clarity. Solid lines are the results of fitting with eq 3.

$0.10$ , and  $0.19$  and to the weight fractions  $w = 0.56, 0.72$ , and  $0.84$ , respectively). The experiment was performed as a function of temperature starting from the melting point of each sample up to  $400\text{ K}$ . During each run the temperature was controlled to the precision of  $\pm 0.1\text{ K}$ . The linearly polarized unimode line ( $\lambda_0 = 532\text{ nm}$ ) of a Coherent DPSS 532 laser, working at a mean power of about  $100\text{ mW}$ , was used as the probe. In each measurement, the VV component of scattered light was collected in the backscattering geometry ( $\theta = 180^{\circ}$ ) and analyzed by a Sandercock-type  $(3 + 3)$ -pass Tandem Fabry–Perot interferometer with a finesse, estimated by the line width of the elastic line, of about  $80$ . The Brillouin peak positions, in the whole composition and temperature range analyzed, were changing between  $7$  and  $15\text{ GHz}$ . The optimum resolution was achieved by setting the cavity length of the interferometer to  $7.5\text{ mm}$ , which corresponds to a free spectral range (FSR) of  $20\text{ GHz}$ . In Figure 2 the experimental Brillouin spectra obtained for pure PEG400 and PEGDME400 at  $298\text{ K}$  are reported as an example.

The recorded spectra were fitted with the convolution of the experimental elastic scattering profile with the following expression:<sup>14</sup>

$$I_{\text{VV}}(\omega) = \delta_{\text{R}} + A_{\text{B}} \left[ \frac{\Gamma_{\text{B}}}{[\omega - \sqrt{\omega_{\text{B}}^2 - \Gamma_{\text{B}}^2}]^2 + \Gamma_{\text{B}}^2} + \frac{\Gamma_{\text{B}}}{[\omega + \sqrt{\omega_{\text{B}}^2 - \Gamma_{\text{B}}^2}]^2 + \Gamma_{\text{B}}^2} \right] + \frac{A_{\text{B}} \Gamma_{\text{B}}}{\sqrt{\omega_{\text{B}}^2 - \Gamma_{\text{B}}^2}} \left[ \frac{\omega + \sqrt{\omega_{\text{B}}^2 - \Gamma_{\text{B}}^2}}{[\omega + \sqrt{\omega_{\text{B}}^2 - \Gamma_{\text{B}}^2}]^2 + \Gamma_{\text{B}}^2} - \frac{\omega - \sqrt{\omega_{\text{B}}^2 - \Gamma_{\text{B}}^2}}{[\omega - \sqrt{\omega_{\text{B}}^2 - \Gamma_{\text{B}}^2}]^2 + \Gamma_{\text{B}}^2} \right] \quad (3)$$

The first term ( $\delta_{\text{R}}$ ) in the above equation describes the central Rayleigh line. The next two terms describe the symmetric contributions to the Brillouin scattering profile ( $A_{\text{B}}$ ,  $\Gamma_{\text{B}}$ , and  $\omega_{\text{B}}$  are the intensity, the half-width at half-maximum (hwhm), and the Brillouin line shift, respectively), whereas the last two terms represent the asymmetric contributions, arising from the first moment preservation selection rule. Continuous lines in Figure 2 represent the best fit results. The fitting procedure furnished the values of the frequency shifts,  $\omega_{\text{B}}$ , with the accuracy better than  $1\%$ , whereas the uncertainty of Brillouin line hwhms,  $\Gamma_{\text{B}}$ , was below  $3\%$ .

The values of the fitting parameters, together with those of the refractive indices and densities, were used to calculate the

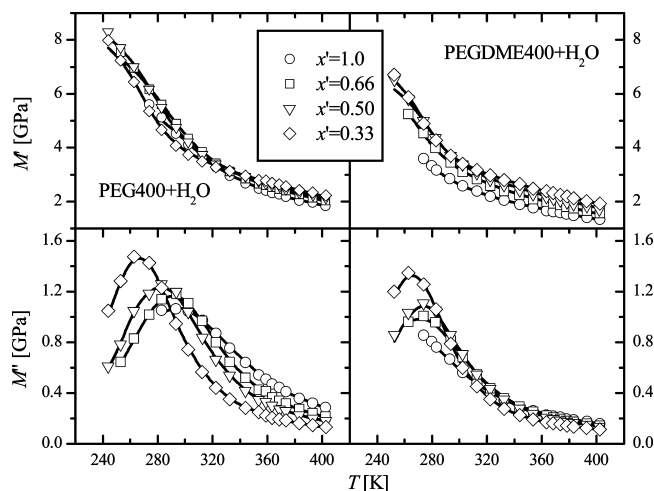


**Figure 3.** Temperature behavior of real and imaginary part of the complex longitudinal modulus for pure PEG400 and PEGDME400 and their aqueous solutions with different concentrations expressed in monomer molar fraction,  $x'$ . Solid lines are the best fit results with eq 8.

values of the real and imaginary parts of the complex longitudinal modulus<sup>14–17</sup>

$$\begin{aligned} M' &= \rho v_B^2 \\ M'' &= \frac{2\Gamma_B}{\omega_B} M' \end{aligned} \quad (4)$$

In eq 4,  $v_B$  is the longitudinal sound velocity which is calculated using the relation

$$v_B = \omega_B / q \quad (5)$$

where  $q = (4\pi n / \lambda_0) \sin(\theta/2)$  is the amplitude of the exchanged wave vector,  $\lambda_0$  is the incident wavelength, and  $\theta$  is the scattering angle.

The temperature dependencies of  $M'$  and  $M''$  for pure PEG400 and PEGDME400 and for their aqueous solutions are presented in Figure 3.

### 3. Results and Preliminary Considerations

An inspection of Figure 3 allows us to make some preliminary comments about the temperature dependencies of longitudinal modulus obtained for aqueous solutions of PEG and PEGDME molecules. A maximum in the loss modulus  $M''$ , occurring at the same temperature where the storage modulus  $M'$  shows an inflection point, can be related to a relaxation process taking place on the picosecond time scale.<sup>18,19</sup> The relaxation time of this process was found independent of the polymeric chain length,<sup>5,6</sup> showing that the molecular dynamics affecting Brillouin spectra involves motion of very few segments.<sup>9</sup> The relaxation process was associated with conformational isomerization dynamics related to the hindered rotation of the C–O–C bonds within the PEG chain.<sup>48</sup> The maximum of the loss modulus,  $M''$ , occurs at the same temperature,  $T_{\max}$ , for different oligomers<sup>48</sup> which suggests the molar mass independence of the relaxation time for PEG. However, the crystallization temperature of the polymeric liquid and its glassy properties depend strongly on the molar mass. Short molecules (PEG200) can be easily supercooled ( $T_{\text{melt}} = 236$  K), whereas very long polymers melt at about 340 K and cannot be supercooled. Note that in this case  $M''$  peak would occur at  $T_{\max} < T_{\text{melt}}$ , so it cannot be observed. PEG400 crystallizes at about 270 K, which is the lowest temperature for this sample reported in Figure 3. Below

this temperature, our samples separate into the crystalline and amorphous phases which differ in refractive index. As a result, samples become opaque and further light scattering experiment is impossible. As follows from the solid–liquid phase diagram of the PEG/water solutions,<sup>5,9,11</sup> when the polymer is dissolved in water, the melting temperature decreases. This allowed us to extend the measurements of mixtures to lower temperatures. Figure 3 unambiguously shows that in PEG400/H<sub>2</sub>O mixtures the maximum position,  $T_{\max}$ , of  $M''(T)$  gradually shifts to lower temperatures as the amount of water increases. A very similar result has been observed for mixtures of PEG600 in different organic solvents<sup>18,19</sup> and in water,<sup>4</sup> as well as for many other moderately viscous polymers or polymeric solutions.<sup>20–23</sup> On the contrary, such behavior is not clearly observed for PEGDME400/H<sub>2</sub>O solutions. This observation demonstrates that substitution of the polymer terminal groups and/or the change of the solution concentration affects the high-frequency dynamics of the samples under investigation, leading to changes in their relaxation behavior. However, some caution should be taken when dealing with this last point. The adopted experimental procedure, i.e., exploring the systems as a function of temperature, implies that each point in  $M'(T)$  and  $M''(T)$  curves reported in Figure 3 is calculated at a different frequency value, namely the Brillouin shift frequency  $\omega_B(T)$ . As a consequence, the quantities  $M'(T)$  and  $M''(T)$  (related to the first and second moments of the spectral distribution through eqs 4 and 5) should be strictly considered as  $M'[\omega_B(T), T]$  and  $M''[\omega_B(T), T]$ . Due to this fact, it is quite evident that several concomitant effects can contribute to the apparent temperature dependence of the complex modulus.

To analyze the observed relaxation process, we have to find a theoretical formalism appropriate for the description of the experimental temperature dependencies of the acoustic parameters. The linear viscoelastic theory can be a suitable approach as long as the viscosity of the system does not assume too high values.<sup>14</sup> In this framework, the dynamical structure factor,  $S(q, \omega)$ , describing the Brillouin scattering profile

$$S(q, \omega) = \frac{I_0}{\omega} \frac{M''(\omega) + \omega \eta_L}{\left[ \omega^2 \frac{\rho}{q^2} - M'(\omega) \right]^2 + [M''(\omega) + \omega \eta_L]^2} \quad (6)$$

depends on both the real and imaginary part of the complex longitudinal relaxation modulus  $M^*(\omega)$ . In eq 6,  $\eta_L$  is the longitudinal viscosity and  $I_0$  is the incoming intensity (for  $\omega \approx \omega_B$ , eq 6 reduces to the shifted Lorentzian contribution appearing in our eq 3). The complex modulus acts as a proportionality factor between longitudinal stress and resulting strain. Its real (in-phase) component  $M'$  describes the ability of the fluid to accumulate elastic energy, while the value of the imaginary (out-of-phase) component  $M''$  is a measure of the energy dissipation.<sup>14,17</sup>

Generally, a relaxation process takes place with a certain relaxation time distribution  $g(\tau)$ . As a consequence, the complex longitudinal relaxation modulus  $M^*(\omega)$  can be written as<sup>16</sup>

$$\begin{aligned} M^*(\omega) &= M' + iM'' = M_\infty - \\ &\quad (M_\infty - M_0) \int_0^\infty g(\tau) \frac{i\omega\tau}{1 + i\omega\tau} d\tau \end{aligned} \quad (7)$$

where  $M_0$  and  $M_\infty$  are the zero and infinite frequency limits of the modulus. At zero frequency the system looks like a fully relaxed fluid, while at infinite frequency it behaves like an elastic medium. The terms “zero” and “infinite” frequency are intended to refer to the frequency position of a given relaxation process with respect to the time window accessible to the experiment.



The adoption of eq 7 implies a difficulty in determining the relaxation time distribution function,  $g(\tau)$ , for a given process over the appropriate time range. A typical approach consists in describing the relaxation function in terms of a semiempirical equation. The Havriliak–Negami relation<sup>24</sup> can be a good approximation for relaxation processes at temperatures higher than the glass transition temperature,  $T_g$ . In such representation, the longitudinal modulus can be written as

$$M^*(\omega) = M_\infty - \frac{M_\infty - M_0}{[1 + (i\omega\tau)^\beta]^\alpha} \quad (8)$$

where  $\tau$  is the mean relaxation time, while  $\alpha$  and  $\beta$  are the shape parameters ( $0 < \alpha, \beta \leq 1$ ) connected with the width of  $g(\tau)$ . When one of the shape parameters (or both) approaches unity, eq 8 reduces to one of the three standard models for the relaxation function: the Debye ( $\alpha = 1, \beta = 1$ ), the Cole–Cole ( $\alpha = 1, 0 < \beta \leq 1$ ) and the Cole–Davidson ( $0 < \alpha \leq 1, \beta = 1$ ) distributions, respectively.

The choice of the relaxation function for the description of a system deeply depends on the experimental conditions. Two distinct effects contribute to the measured temperature dispersion of the relaxation. The first one is the rate of change of the relaxation time with temperature. The lower this rate is, the wider is the temperature range over which the process will be observed within the experimental time window. As a consequence, the  $M''$  plots reported in Figures 3 exhibit peaks whose widths reflect the rate of  $\tau(T)$ . The second factor which can affect the temperature dispersion of  $M^*(\omega)$  is the width of the relaxation distribution function. Also in this case the process characterized by a broader distribution function will be observed, within a given frequency window, over a wider temperature range. It is then clear that, for any model involving both the above-mentioned factors, some of these parameters will be strongly correlated.

The wide suitability of the general form of eq 8 in reproducing many relaxation processes stems from the fact that the Havriliak–Negami phenomenological function interpolates two power law regimes, often observed in complex systems. Its shape parameters are the exponents of these power laws. At frequencies lower than relaxation frequency  $M''(\omega) \propto \omega^{-\beta}$ , whereas at higher frequencies  $M''(\omega) \propto \omega^{-\alpha\beta}$ . Depending on the probe frequency and on the actual temperature of the system, the low- or the high-frequency side of the longitudinal modulus will be measured. It is now clear how the choice of the adequate model for the relaxation process description depends on the temperature range of the experiment. In general, for wide temperature range experiments, the Havriliak–Negami function should be used while the use of the Debye function could be a suitable choice when narrow temperature ranges are explored.

#### 4. Fitting Procedure

Each parameter in eq 8 is temperature dependent and this dependence has to be obtained from additional measurements or assumed on the basis of ad hoc considerations. The temperature dependence of the relaxed value of the longitudinal modulus,  $M_0 = \rho \cdot v_0^2$ , has been calculated from the high temperature values of the measured hypersonic velocity, assumed as a low-frequency velocity,  $v_0$ . The limited  $(\omega, T)$  region accessible to our experiment did not allow us to register unrelaxed values of the modulus. Several approaches could be adopted in order to assume a suitable behavior for  $M_\infty(T)$ .<sup>23,44</sup> The estimate of the  $M_\infty(T)$  under the assumption of a linear temperature dependence of  $v_\infty$  is, in our opinion, the safest procedure. Even supposing that this assumption could be not

strictly correct, we can be confident that any deviation from linearity should be negligible over the limited temperature range explored (this assumption for  $v_\infty$  implies a nonlinear temperature dependence of  $M_\infty$ , in agreement with literature indication<sup>23,44</sup>). The slope of  $v_\infty$  has been fixed equal to that of  $v_0$  (due to the limited temperature range, this further assumption should not give rise to significant errors). In such a way, only one parameter (namely the value of  $v_\infty$  at  $T = 0$ ) is involved in the calculation of  $M_\infty(T)$  through eq 4.

The other fit parameters are related to the temperature dependence of the relaxation time,  $\tau(T)$ . The universal picture of relaxing dynamics in polymers assumes the existence of two distinct regimes: a high-temperature regime, where the system is dominated by a single relaxation process, and a low-temperature regime, where two distinct processes are observed.<sup>5,22,23,25</sup> Dielectric spectroscopy measurements show that this scenario applies also for supercooled ethylene glycol oligomers water mixtures<sup>12</sup> as well as for higher molecular weight compounds like PEG200, PEG600, and PEG6000 and their aqueous solutions.<sup>5,6</sup> In many polymeric liquids, the single relaxation process at high temperatures follows simple Arrhenius dependence and the deviation starts to be observed for supercooled samples only. However, in PEG samples, a non-Arrhenius dependence of a high-frequency process was already observed at high temperatures by dielectric spectroscopy.<sup>5,45</sup>

When the Arrhenius law was assumed for  $\tau(T)$ , our experimental data could not be fitted even with the Havriliak–Negami model (eq 7) for any set of parameters. This result, together with the previous dielectric findings, justifies the use of the Vogel–Fulcher–Tamman (VFT) equation<sup>26</sup> for  $\tau(T)$ :

$$\tau(T) = \tau_0 \exp\left(\frac{DT_0}{T - T_0}\right) \quad (9)$$

Equation 9 is commonly adopted to describe the relaxation dynamics of glass formers. In this equation,  $\tau_0$  is the high-temperature limit of the fast relaxation and  $T_0$  represents the temperature at which the average value of the relaxation time diverges. The coefficient  $D$  can be regarded as a measure of the system fragility. The lower its value is, the larger the departure from Arrhenius behavior (the more fragile sample) is.<sup>13,27,28</sup>

With the adoption of the VFT model, the simple Debye function turned out to be too narrow to produce a good fit of the experimental data. Of course, the Havriliak–Negami function fits the data almost perfectly. This is not surprising, due to larger number of parameters. However, in such a case a strong correlation among the values of the parameters has been detected and the Havriliak–Negami model is unable to produce unambiguous fitting results. As a compromise, the Cole–Cole function has been suggested as an appropriate description of the relaxation processes in our case.

The continuous lines in Figure 3 represent the fitting results obtained using eq 8 with  $\alpha = 1$ . The sets of the fit parameters values are reported in Table 1.

The additional advantage of using the Cole–Cole function stems from the fact that it is the Fourier transform of the Kohlrausch–William–Watts (KWW) stretched exponential

$$f(t) = \exp(-t/\tau)^\beta \quad (10)$$

where  $\beta$  is always less than or equal to unity and contains information about the width of the distribution. Moreover, recent dielectric measurements of systems similar to those investigated in this paper have shown that the Cole–Cole function is a good description of the high-frequency dielectric relaxation process.<sup>12,29</sup>

**TABLE 1: Outcomes of the Fitting Procedure Adopted to Experimental Data from Aqueous Solutions with Different Monomer Molar Fractions ( $x'$ ) of PEG400 and PEGDME400<sup>a</sup>**

$x'$	$\tau_0$ (fs)	$T_0$ (K)	$D$	$\beta$	$a$ (m·s <sup>-1</sup> )	$b$ (m·s <sup>-1</sup> ·K <sup>-1</sup> )
PEG400 + H <sub>2</sub> O						
1.00	129.3	157.6	4.16	0.779	2540.2	-3.0
0.67	125.6	156.5	4.11	0.778	2879.6	-3.7
0.50	51.6	152.0	4.73	0.753	2597.5	-2.9
0.33	17.2	143.0	5.59	0.819	2826.7	-3.4
PEGDME400 + H <sub>2</sub> O						
1.00	6.9	145.0	6.37	0.696	2239.1	-2.7
0.67	1.7	145.0	7.76	0.665	2578.7	-3.3
0.50	0.8	145.0	8.27	0.646	2619.4	-3.2
0.33	0.2	141.5	9.35	0.679	2699.5	-3.2

<sup>a</sup>Symbols are explained in text. The last two columns on the right represent the coefficients of the linear regression of the low-frequency sound velocity dependence on the temperature:  $v_0 = a + bT$ .

## 5. Discussion

Brillouin scattering measurements on poly(propylene glycol) (PPG) of different molecular weight<sup>22</sup> have shown that the nature of the terminal groups plays a relevant role for short chains while it has almost no influence on long polymers. In particular, the data for OH-capped PPG are nearly independent of the chain length while a strong dependence of the  $M''(T)$  peak position on the PPG chain length was found for CH<sub>3</sub>-capped polymers. This observation was attributed to the effect of transient cross-links. OH-terminated systems exhibit an effective molecular weight larger than a single polymeric chain. The different concentration dependence of the  $M''(T)$  peak position, obtained in the present work and reported in Figure 3, can be consistently interpreted. For OH-capped molecules (PEG), the effective molecular weight of the sample seems to be higher than the molecular weight of the individual molecule. The established H-bonded network appears as a stable structure if investigated on a time scale shorter than its lifetime.<sup>30</sup> The observed shift of the maximum position toward lower temperature, observed for OH-capped polymers, agrees with the idea of an effective chain length which decreases upon dilution.

A peak position which appears almost independent of the concentration, as observed for PEGDME400/H<sub>2</sub>O mixtures, can be related to the different structure of hydrogen-bond network in the case of CH<sub>3</sub>-capped sample. In fact, looking carefully at Figure 3, one can guess that  $M''(T)$  peak position for pure PEGDME is located at a lower temperature than those observed in its concentrated solutions. Pure PEGDME is a nonassociated liquid because its molecules possess only hydrogen-bond acceptors without any donor. H-bonds in the system are formed only after introduction of some amount of water. When the proportion between hydrogen-bond donors and acceptors present in the system increases, the degree of association increases as well, causing the molecular motions to slow down. According to wait-and-switch model,<sup>29,31</sup> when the concentration of H-bonds in the system reaches a high enough value, local destabilization of the network structure may occur, leading to shortening of the molecular reorientation times.

The result of a single fast relaxation process taking place on a time scale of 10 ps is consistent with the results of Brillouin scattering measurements on PEG200 and PEG400<sup>20,32,33</sup> and with our previous findings from PEG600 and its solutions in some organic solvents.<sup>18,19</sup> The observed relaxation motion can be definitely related to the polymeric component and can be

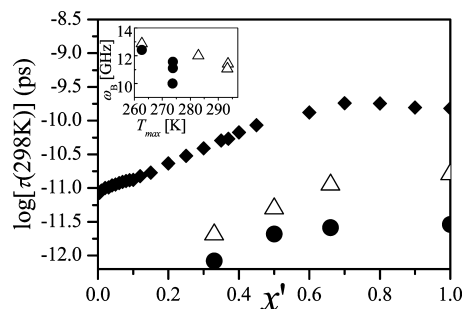


**Figure 4.** Concentration dependence of relaxation times for aqueous solution of PEG400 and PEGDME at  $T = 298$  K. Diamonds represent the dielectric relaxation times for PEG400, taken from ref 25. Circles and triangles are the values obtained in this work.

assigned to conformational rearrangements of the polymeric chains. It should be noted that the relaxation times measured by our experiment appear to be an order of magnitude faster than the relaxation time measured by dielectric spectroscopy in the gigahertz region in analogous systems.<sup>5,7,8</sup> This could indicate that the relaxation of the polymeric solutions under mechanical stresses is much faster than the relaxation under electrical stresses. A similar discrepancy between the results from the two techniques<sup>22,34</sup> has been sometimes attributed to different relaxing quantities measured in the two cases.<sup>35</sup> The fact that the relaxation times revealed by the two techniques seem to exhibit the similar behavior as a function of polymer concentration (see Figure 4) suggests that the same microscopic process is driving the observed different relaxations. This idea can be further supported by the occurrence that a change of the slope in the  $\log \tau$  vs  $x'$  curves is observed around the same concentration with no respect of the experimental technique.

The values of the parameter  $D$  reported in Table 1 definitely indicate that PEGDME400 is a *stronger* system than PEG400. In both cases the addition of small quantities of water results in the progressive decrease of the system fragility. For all the investigated systems the obtained values of the KWW exponent  $\beta$  suggest the presence of a relatively broad distribution of relaxation times.

Of course, while the values of the obtained relaxation times (see Figure 4) can be assumed to be significant, the meaning of the involved parameters should be taken with some caution. We emphasize that in our study the VFT equation was just a phenomenological relation adopted to describe a relaxation process which fails to follow the simple Arrhenius law.

In particular, the meaning of the  $T_0$  temperature is not easily understandable. Since for  $T = T_0$  the relaxation time diverges,  $T_0$  can be assumed as an indication of the temperature for which a structural arrest takes place. From such perspective,  $T_0$  can be related to the glass transition temperature,  $T_g$ . Dielectric experiments on OH-terminated PPG have shown a very weak dependence of the  $\alpha$ -relaxation time and of  $T_g$  on the polymer chain length.<sup>36–38</sup> On the contrary, for the CH<sub>3</sub>-capped PPG, an initial increase of  $T_g$  with molecular weight has been found, which finally saturates for high molecular weight polymers, reaching a value that becomes independent of the polymer end group.<sup>22</sup> The calorimetric experiments have shown molecular weight dependence of  $T_g$  for the short-chain PEGs.<sup>11,39</sup> For concentrated aqueous solutions of PEG (OH capped) it was found<sup>11,40</sup> that  $T_g$  is apparently independent of water content. This weak dependence of  $T_g$  both on molecular weight and concentration suggests that a relevant role is played by the H-bonds in the formation of a supermolecular structure which dominates the macroscopic properties of the systems. The

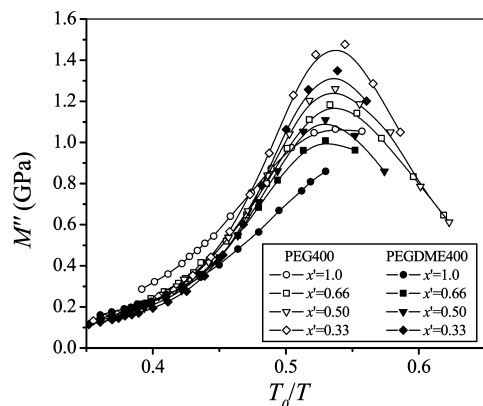


**Figure 5.**  $M''(T)$  curves for pure PEG400 and PEGDME400 and their aqueous solution, reported as a function of the reduced temperature (see text for details).

existence of solute/solvent complexes in PEG/water solutions has been suggested to explain nontrivial concentration dependence of  $T_g$ .<sup>46</sup>

Interestingly, our  $T_0$  values are somehow correlated with the corresponding calorimetric  $T_g$  values, at least for PEG400/water mixtures for which  $T_g$  values are available.<sup>46,47</sup> Even if our  $T_0$  values are too low to be directly related to the glass transition temperatures, the value of  $T_0 - T_g$  for each mixture is nearly a constant ( $\sim 40$  K). It is surprising that the  $T_0$  values obtained from high-temperature experiment ( $T > T_g + 100$  K) correlates so well with the glass transition temperatures. The existence of such a correlation suggests that the observed relaxation process follows the same temperature dependence (the VFT type in this case) starting from high temperatures down to  $T_g$ . The recent scenario of the relaxation processes in aqueous solutions of oxyethylene glycol oligomers predicts such a behavior.<sup>45</sup> In the low-water-content mixtures with large solute and at low enough temperatures, the process observed is mainly caused by the cooperative motion of polymeric molecules and their surrounding water molecules.

An interesting feature is revealed if the experimental  $M''(T)$  values are reported as a function of the reduced inverse temperature,  $T_0/T$  (see Figure 5). Such a result can be an indication of a self-similar behavior of the relaxation time distribution or of the relaxation time temperature dependence. In such a perspective, both  $g(\tau)$  and  $\tau(T)$  should be described in terms of appropriate power laws.<sup>41</sup> Very recently, a comparison of numerical simulations and experimental results suggested the existence of an universal scaling law between structural relaxation and vibrational dynamics in glass-forming liquids and polymers.<sup>42</sup> Since a relation with vibrational dynamics, i.e., with the Debye–Waller factor, means a relation with temperature, the analogy with the above-reported results is almost immediate.

However, we have to remember that the approach defined in terms of fragile and strong liquids has been formulated for glass-forming and/or supercooled liquids. As a consequence, it can be safely applied to pure molten PEG400 and PEGDME400 but any extended analogy to include their aqueous solutions requires some caution. Nevertheless, it seems reasonable to assume that the addition of small quantities of water does not destroy the original local structure of molten polymers that is likely preserved by hydrogen-bond interactions. Some hints toward such a picture can be obtained from Figure 4. The addition of small quantities of water to pure polymer does not seem to cause any decrease of the relaxation time until a critical

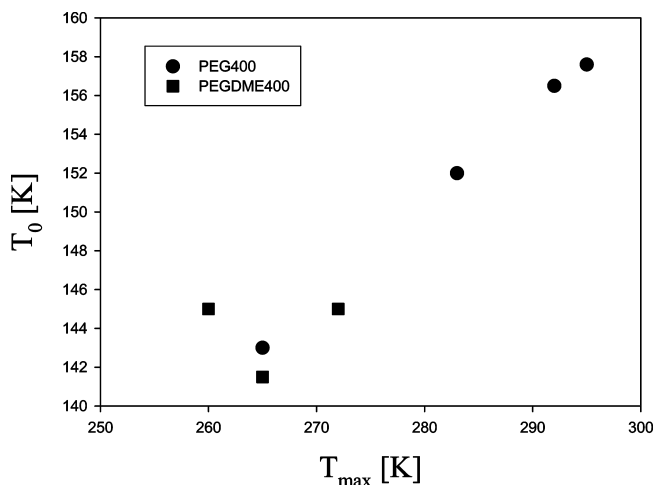


**Figure 6.** Plot of  $T_0$  (as obtained by the fitting procedure) vs  $T_{\max}$  (the temperature where the maximum of each  $M''$  curve is located).

concentration is reached (this can be easily observed from the dielectric data). A similar behavior can be guessed for PEGDME400, with the change of slope probably located at lower  $x'$  values. This last observation is clearly over the range of our actual results, and the acquisition of further experimental points at different temperature values is required for a safe discussion of the point. If confirmed, the difference between PEG400 and PEGDME400 could be the result of an unusual solvent effect already observed in PEGDME aqueous solutions.<sup>43</sup> In both cases, the molecular motion is strongly affected by the formation of H-bonds between solvent and solute. The effect starts to be evident at lower water contents for  $\text{CH}_3$ -capped polymer since no H-bonds are present in the pure system.

For PEGDME the  $x' = 0.5$  concentration corresponds to the situation where each water molecule hydrates one ethylene oxide group. As the water molecule donates two H-bonds and the ether oxygens in polymeric chain can accept two H-bonds, the equimolar composition sample can be considered as a transient gel where each water molecule acts as a cross-link between ethylene oxide groups. It is less important if the two bridged ethylene oxide groups belong to the same or to two neighboring polymer molecules. As far as the polymeric chains are long enough, these two situations are indistinguishable. The effective molecular weight of such cross-linked structure is much higher than that of a single chain and is independent of both the polymer chain length and its end groups. Within this scenario, such considerations could be enough to rationalize the observed higher fragile character of PEG400 and its aqueous solutions.

## 6. Concluding Remarks

To our best knowledge, the  $T_g$  values for PEGDME/water different mixtures are not available. For this reason, even if some correlation between  $T_0$  and  $T_g$  has been observed for the PEG/water system, it is not clear if we can extrapolate this observation for PEGDME aqueous solutions. In such a framework the meaning of  $T_0$  should be rather that of a scaling parameter, introduced just for a phenomenological description, to which no physical meaning should be assigned. It seems that this parameter accounts for the temperature shift of the  $M''$  curve when the amount of water increases. This is supported by Figure 6 where a correlation between  $T_0$  and  $T_{\max}$  (temperature at  $M''$  maximum position, Figure 3) is observed for each sample but pure PEGDME400. This can indicate that for all the samples on the straight line in Figure 6 we observe a relaxation process of



the hydrogen-bonded network in which both the polymer component and water play a role. The fact that the same scaling holds well for polyethylene oxides mixtures, independent of the termination of the polymer, suggests that the observed relaxations are related to rearrangements of very similar local structures. In such a picture, water works as a “stabilizer” able to act as a cross-linker between polymer chains. When the relative amount of the polymeric chains decreases in the system, as a result of water addition, the concentration of the relaxing entities drops. This has been interpreted as the source of the apparent decrease of the effective chain length reflected in the observed shift of the  $M''$  curves toward lower temperatures, when the water content increases (Figure 3). This behavior looks independent of the dissolved polymeric species as long as the H-bond connectivity of the network is already established. The difference in the results obtained for mixtures of polymers with different termination groups concerns the situation where the amount of water (cross-linker) is very low and arises from the different hydrogen-bond connectivity present in both cases. Particularly, different amounts of water need to be introduced into the polymeric liquid of a given type, in order to obtain hydration structure of the same H-bond connectivity.

Summing up, we observe in PEG and PEGDME aqueous solutions a relaxation process involving the motion of the same complex structure and occurring at different concentration. In addition, the dilution of the structure apparently changes its effective chain length and, finally, the  $T_0/T$  form of the adopted scaling removes the effective chain length dependence from the  $M''(T)$  data.

## References and Notes

- (1) Alberts, B.; Bray, D.; Lewis, J.; Raff, M.; Roberts, K.; Watson, J. D. *Molecular Biology of the Cell*; Garland Publishing, Inc.: New York, 1994.
- (2) Schrödinger, E. *What is Life? The Physical Aspect of the Living Cell*; Cambridge University Press: Cambridge, UK, 1967 (reprinted).
- (3) Prigogine, I. *From Being to Becoming*; Freeman: San Francisco, 1980.
- (4) Pochylski, M.; Aliotta, F.; Błaszczak, Z.; Gapiński, J. *J. Phys. Chem. B* **2006**, *110*, 20533.
- (5) Murthy, S. S. N. *J. Phys. Chem. B* **2000**, *104*, 6955.
- (6) Tyagi, M.; Murthy, S. S. N. *Carbohydr. Res.* **2006**, *341*, 650.
- (7) Sato, T.; Niwa, H.; Chiba, A.; Nozaki, R. *J. Chem. Phys.* **1998**, *108*, 4138.
- (8) Shinyashiki, N.; Asaka, N.; Mashimo, S.; Yagihara, S. *J. Chem. Phys.* **1990**, *93*, 760.
- (9) Derkaoui, N.; Said, S.; Grohens, Y.; Olier, R.; Provat, M. *J. Colloid Interface Sci.* **2006**, *305*, 330.
- (10) Hatakeyama, T.; Kasuga, H.; Tanaka, M.; Hatakeyama, H. *Thermochim. Acta* **2007**, *465*, 59.
- (11) Huang, L.; Nishinari, K. *J. Polym. Sci. B: Polym. Phys.* **2001**, *39*, 496.
- (12) Sudo, A.; Tsubotani, S.; Shimomura, M.; Shinyashiki, N. *J. Chem. Phys.* **2004**, *121*, 7332.
- (13) Angell, C. A. *J. Phys. Solids* **1988**, *49*, 863.
- (14) Boon, J. P.; Yip, S. *Molecular hydrodynamics*; McGraw-Hill: New York, 1980.
- (15) Aliotta, F.; Ponterio, R.; Salvato, G.; Musso, M. *J. Phys. Chem. B* **2004**, *108*, 732.
- (16) Ferry, J. D. *Viscoelastic Properties of Polymers*, 3rd ed.; Wiley: New York, 1984.
- (17) Montrose, C. J.; Solov'yev, V. A.; Litovitz, T. A. *J. Acoust. Soc. Am.* **1968**, *43*, 131.
- (18) Pochylski, M.; Aliotta, F.; Błaszczak, Z.; Gapiński, J. *J. Phys. Chem. B* **2005**, *109*, 4181.
- (19) Pochylski, M.; Aliotta, F.; Błaszczak, Z.; Gapiński, J. *J. Phys. Chem. B* **2006**, *110*, 485.
- (20) Wang, C. H.; Li, B. Y.; Rendell, R. W.; Ngai, K. L. *J. Non-Cryst. Solids* **1991**, *131*, 870.
- (21) Wang, C. H.; Fytas, G.; Zhang, J. *J. Chem. Phys.* **1985**, *82*, 3405.
- (22) Engberg, D.; Schüller, J.; Strube, B.; Sokolov, A. P.; Torrell, L. M. *Polymer* **1999**, *40*, 4755.
- (23) Lehman, S. Y.; McNeil, L. E.; Albalak, R. *J. Polym. Sci.* **2000**, *38*, 2170.
- (24) Havriliak, S.; Negami, S. *J. Polym. Sci. C* **1966**, *14*, 99.
- (25) Murthy, S. S. N.; Sobhanadri, J.; Gangasharan, J. *J. Chem. Phys.* **1994**, *100*, 4601.
- (26) Vogel, H. *Phys. Z.* **1921**, *22*, 645.
- (27) Adam, G.; Gibbs, J. H. *J. Chem. Phys.* **1965**, *43*, 139.
- (28) Gibbs, J. H. *Modern Aspects of the Vitreous State*; Butterworth: London, 1960.
- (29) Hanke, E.; von Roden, K.; Kaatz, U. *J. Phys. Chem. B* **2006**, *125*, 084507.
- (30) Vergara, A.; Paduano, L.; Capuano, F.; Sartorio, R. *Phys. Chem. Chem. Phys.* **2002**, *4*, 4716.
- (31) Kaatz, U.; Behrends, R.; Pottel, R. *J. Non-Cryst. Solids* **2002**, *305*, 19.
- (32) Wang, C. H.; Lin, Y.-H.; Jones, D. R. *Mol. Phys.* **1979**, *37*, 287.
- (33) Noudou, T.; Matsuoka, T.; Koda, S.; Nomura, H. *Jpn. J. Appl. Phys.* **1996**, *35*, 2944.
- (34) Pochylski, M.; Aliotta, F.; Błaszczak, Z.; Gapiński, J. *Macromol. Symp.* **2007**, *251*, 47–53.
- (35) Fioreto, D.; Comez, L.; Socino, G.; Veridini, L.; Corezzi, S.; Rolla, P. A. *Phys. Rev. E* **1999**, *59*, 1899.
- (36) Heinrich, G. *Polymer* **1988**, *29*, 1198.
- (37) Jacobsson, P. *J. Non-Cryst. Solids* **1991**, *131*, 104.
- (38) Melnichenko, Y. B. *J. Chem. Phys.* **1995**, *103*, 2016.
- (39) Craig, D. Q. M. *Thermochim. Acta* **1995**, *248*, 189.
- (40) Hatakeyama, T.; Kasuga, H.; Tanaka, M.; Hatakeyama, H. *Thermochim. Acta* **2007**, *465*, 59.
- (41) Martinez, L. -M.; Angell, C. A. *Nature* **2001**, *410*, 663.
- (42) Larini, L.; Ottochian, A.; De Michele, C.; Leporini, D. *Nat. Phys.* **2008**, *4*, 42.
- (43) Shikata, T.; Takahashi, R.; Sakamoto, A. *J. Phys. Chem. B* **2006**, *110*, 8941.
- (44) Floudas, G.; Fitas, G.; Alig, I. *Polymer* **1991**, *32*, 2307.
- (45) Sudo, S.; Shinyashiki, N.; Arima, Y.; Yagihara, S. *Phys. Rev. E* **2008**, *78*, 011501.
- (46) Murthy, S. S. N. *Cryobiology* **1998**, *36*, 84.
- (47) Murthy, S. S. N.; Singh, G. *Thermochim. Acta* **2008**, *469*, 116.
- (48) Wang, C. H.; Lin, Y. H.; Jones, D. R. *J. Mol. Phys.* **1979**, *37*, 287.

JP9052456